Oxygen isotopic diversity of chondrule precursors and the nebular origin of chondrules

Yves Marrocchi, Johan Villeneuve, Valentina Batanova, Laurette Piani, Emmanuel Jacquet

Oxygen isotopic diversity of chondrule precursors and the nebular origin of chondrules

Yves Marrocchi[1,*], Johan Villeneuve[1], Valentina Batanova[2], Laurette Piani[1] and Emmanuel Jacquet[3]

[1]CRPG, CNRS, Université de Lorraine, UMR 7358, Vandoeuvre-lès-Nancy, 54501, France. [2]Université Grenoble Alpes, ISTerre, CNRS, UMR 5275, Grenoble, F-38000, France. [3]IMPMC, CNRS & Muséum national d'Histoire naturelle, UMR 7590, CP52, 57 rue Cuvier, 75005 Paris, France

Correspondence: *yvesm@crpg.cnrs-nancy.fr

Abstract

FeO-poor (type I) porphyritic chondrules formed by incomplete melting of solid dust precursors *via* a yet-elusive mechanism. Two settings are generally considered for their formation: (i) a nebular setting where primordial solids were melted, e.g. by shock waves propagating through the gas and (ii) a collisional planetary setting. Here we report a method combining high-current electron microprobe X-ray mapping and quantitative measurements to determine the chemical characteristics of relict olivine grains inherited from chondrule precursors. We find that these olivine crystals are Ca-Al-Ti-poor relative to host olivine crystals. Their variable $\Delta^{17}O$, even in individual chondrule, is inconsistent with derivation from planetary interiors as previously argued from 120° triple junctions also exhibited by the

chondrules studied herein. This indicates that chondrule precursors correspond to solid nebular condensates formed under changing physical conditions.

We propose that porphyritic chondrules formed during gas-assisted melting of nebular condensates comprising relict olivine grains with varying $\Delta^{17}O$ values and Ca-Al-Ti-rich minerals such as those observed within amoeboid olivine aggregates. Incomplete melting of chondrule precursors produced Ca-Al-Ti-rich melts (CAT-melts), allowing subsequent crystallization of Ca-Al-Ti-rich host olivine crystals *via* epitaxial growth on relict olivine grains. Incoming MgO and SiO from the gas phase induced (i) the dilution of CAT-melts, as attested by the positive Al-Ti correlation observed in chondrule olivine crystals, and (ii) buffering of the O-isotope compositions of chondrules, as recorded by the constant $\Delta^{17}O$ values of host olivine grains. The O-isotopic compositions of host olivine grains are chondrule-specific, suggesting that chondrules formed in an array of environments of the protoplanetary disk with different $\Delta^{17}O$ values, possibly due to variable solid/gas mixing ratios.

.

Keywords: chondrule, oxygen isotopes, relict olivine, epitaxial growth, gas-melt interactions

1- Introduction

Chondrules (millimeter-sized igneous spheroids containing silicates, metal, sulfides, and glass) are the major high-temperature components of primitive meteorites (chondrites), suggesting that most inner solar system materials were affected by their formation. However, the underlying mechanism(s) of their formation remains a mystery and diverse scenarios are debated in contemporaneous literature. A key clue to their origin would be the identification of the precursor material that was melted to form chondrules. In this effort, cosmochemists may find help in the incomplete melting of most chondrules, as evidenced by their widespread porphyritic texture (Hewins et al., 2005). Indeed, *relict* grains inherited from chondrule precursors are identifiable. Forsteritic grains in high-FeO (type II) porphyritic chondrules were presumably inherited from precursors formed in more reducing conditions than their current host (Nagahara, 1981; Scott and Jones, 1990). Conversely, "dusty" grains, i.e., crystals speckled with Fe-rich metal beads, in low-FeO (type I) chondrules are commonly attributed to oxidized precursors that underwent reduction during formation of their host chondrules (Lemelle et al., 2001; Leroux et al., 2003; Nagahara, 1981; Rambaldi, 1981). These examples represent only a fraction of the existing relicts. In type I chondrules—the dominant type in carbonaceous chondrites and hence the main asteroid belt—relict grains from *reduced* precursors are not so easily recognizable.

Oxygen isotopic systematics may help to identify such relicts (Kimura et al., 2011; Kunihiro et al., 2004, 2005; Rudraswami et al., 2011; Schrader et al., 2013; 2015; Tenner et al., 2013, 2015; Ushikubo et al., 2012). Indeed significant isotopic diversity is observed among solar system materials, from ^{16}O-rich refractory inclusions (calcium-aluminum-rich inclusions (CAIs), amoeboid olivine aggregates (AOA)) to ^{16}O-poorer chondrules (Clayton, 2003). Type I chondrules exhibit significant variability and define a broad line in the oxygen

three-isotope diagram that is not specific to chondrules of a given chondrite or to particular chondrite type and known as the primitive chondrule minerals (PCM) line (Ushikubo et al., 2012). The underlying ^{16}O variability could result from (i) physical mixing of grains of different origins within the solid chondrule precursors (Hezel & Palme, 2007; Tenner et al., 2015) and/or (ii) high-temperature exchanges between the chondrule melt and the surrounding gas (Marrocchi and Chaussidon, 2015). Secondary ion mass spectrometer (SIMS) analyses of olivines within a single chondrule typically reveal homogeneous oxygen isotopic compositions (Chaussidon et al., 2008; Tenner et al., 2015). Yet, in some chondrules, some olivines are ^{16}O-enriched compared to their neighbors (Kunihiro et al., 2005; Rudraswami et al., 2011): these are generally considered to be relict grains, even if they are not petrographically manifest (Ushikubo et al., 2012).

Despite these additions to the known inventory of relict grains, their origin remains unclear. Relict olivine grains could correspond to (i) early condensates from the gas of the solar protoplanetary disk (Cohen et al., 2004; Jacquet and Marrocchi, 2017; Russell et al., 2005; Yurimoto and Wasson, 2002), (ii) collisional debris from early-generation planetesimals (Libourel and Chaussidon, 2011; Libourel and Krot, 2007) and/or (iii) earlier generations of chondrules (e.g., Ruzicka et al., 2007). Progress on the identification of the origin of relict olivine grains is frustrated by our poor understanding of their abundance, distribution and specific chemical compositions (Pack et al., 2005; 2004; Ruzicka et al., 2007). Among isotopic studies, only a few *in situ* measurements of olivine are generally performed within a single chondrule (usually 2–10; Rudraswami et al., 2011), leading to an misestimate of the abundance of relict olivine grains (and relict-bearing chondrules) and a lack of knowledge of their isotopic characteristics. Furthermore, there are no clear major-element signatures and/or textural features that facilitate the recognition of relict olivine grains (Jones et al., 2004; Ushikubo et al., 2012). Consequently, the message carried by relict

olivine grains remains difficult to decipher, however fundamental it would be to understand the origin of chondrules.

Here we report a new method combining high-resolution X-ray maps, electron microprobe analyses, and SIMS oxygen isotope measurements to quantitatively assess for the first time the nature of relict olivine grains in type I chondrules. This method was successfully applied to type I porphyritic chondrules in the CM-related ungrouped chondrite Northwest Africa (NWA) 5958 (Jacquet et al., 2016) and provides new information on the formation conditions of the first solids of the solar system.

2- Material and methods

NWA 5958 is a carbonaceous chondrite found in the Moroccan desert in 2009 that shares numerous similarities with the CM chondrite group. This meteorite shows limited terrestrial weathering and a low degree of aqueous alteration (Jacquet et al., 2016). Its bulk oxygen isotopic composition ($\Delta^{17}O = -4.3‰$) is more ^{16}O-rich than all CM chondrites, further supporting a limited alteration episode (Marrocchi et al., 2018; Verdier-Paoletti et al., 2017). As previous O isotope studies have revealed CO chondrules to be richest in relicts (Tenner et al., in press), this meteorite, as a member of the CM-CO clan, was a sample of choice to increase their chances of discovery.

We surveyed all type I chondrules in thick section NWA 5958-1 (from the Muséum national d'Histoire naturelle collection, Paris, France) of NWA 5958. The X-ray map of NWA5981-1 was reported elsewhere (Fig. 1 of Jacquet et al., 2016). Chondrules were examined microscopically in reflected light. Scanning electron microscope observations were performed at CRPG using a JEOL JSM-6510 with 3 nA primary beam at 15 kV. Among 32 Mg-rich porphyritic Type I chondrules examined, we selected 3 olivine-rich chondrules (Fig.

1, 2, S1−S3). High-resolution X-ray element distribution maps were performed at the Institut des Sciences de la Terre (ISTerre, Grenoble, France), using a JEOL JXA-8230 electron microprobe analyzer (EMPA) equipped with five wavelength-dispersive spectrometers (WDS) and one silicon drift detector energy-dispersive spectrometer (EDS; Batanova et al., 2015). Analysis were performed with an acceleration voltage of 20 kV, beam current of 500 nA, 1.5-μm step size, and dwell time of 500 ms. Al, Ca, Cr, Mn and Ti were measured by WDS while Fe, Si and Mg were measured by EDS. Each map last 24 hours followed by 8 hours of quantitative analyses. Detection limits were below 40 ppm for Al, Ca, Ti, Cr and Mn as estimated from minimum differences between the average concentrations of the visually distinct homogeneous zones and standard deviations of concentration of homogeneous zones. These X-ray maps are semi-quantitative, as the background was not quantified by performing similar off-peak maps. However, quantitative analyses of all olivine grains large enough to be isotopically characterized by SIMS were then performed with the following conditions: accelerating voltage 20 kV, probe current 900 nA, beam diameter 1 μm, and 320 s total peak/background counting time. Such a high current and long counting time allow very low detection limits estimated to be 10 ppm for Al, Ca, Ti, Cr and Mn. The ZAF software was used for matrix corrections (see Batanova et al. 2015 for further details).

We measured the oxygen isotopic compositions of chemically characterized olivine crystals with a CAMECA ims 1270 E7 at CRPG-CNRS (Nancy, France). $^{16}O^-$, $^{17}O^-$, and $^{18}O^-$ ions produced by a Cs^+ primary ion beam (~15 μm, ~4 nA) were measured in multi-collection mode with two off-axis Faraday cups (FC) for $^{16,18}O^-$ and the axial FC for $^{17}O^-$. To remove $^{16}OH^-$ interference on the $^{17}O^-$ peak and to maximize flatness atop the $^{16}O^-$ and $^{18}O^-$ peaks, the entrance and exit slits of the central FC were adjusted to obtain mass resolution power of ~7000 for $^{17}O^-$. The multicollection FCs were set on exit slit 1 (MRP = 2500). Total measurement times were 240 s (180s measurement + 60s pre-sputtering). We used three

terrestrial standard materials (San Carlos olivine, magnetite and diopside) to define the instrumental mass fractionation line for the three oxygen isotopes and correct for instrumental mass fractionation for olivine. To obtain good precision on analytical measurements, we analyzed, in order, 4 standards, 8 chondrule olivine crystals and 4 standards. Typical count rates obtained on the San Carlos olivine standards were 2.5×10^9 cps for ^{16}O, 1.0×10^6 cps for ^{17}O, and 5.4×10^6 cps for ^{18}O. The number of Mg-rich olivines analyzed per chondrule were 45, 45 and 28, with typical uncertainties of 0.2, 0.4 and 0.7‰ for $\delta^{18}O$, $\delta^{17}O$ (measured relative to standard mean ocean water, SMOW, as $\delta^{17,18}O = [(^{17,18}O/^{16}O)_{sample}/(^{17,18}O/^{16}O)_{SMOW} - 1] \times 1000$ ‰), and $\Delta^{17}O$ ($= \delta^{17}O - 0.52 \times \delta^{18}O$), respectively (Table S1).

3- Results

All porphyritic chondrule textural types are present in NWA 5958, i.e., porphyritic olivine-rich (PO), porphyritic olivine-pyroxene (POP), and porphyritic pyroxene-rich (PP); Figs. 1–3). Among the chondrules examined, two PO chondrules (Ch-1 and Ch-7) were chosen for detailed examination. They are characterized by many variably-sized (≈ 30–300 μm) subhedral to euhedral olivine grains meeting in 120° triple junctions (Figs. 1, 2, S1–S2) first described by (Libourel and Krot, 2007), altered mesostases, and Fe-Ni metal beads (Figs. 1, 2A, and S1–S2). Large, euhedral low-Ca pyroxenes surround both chondrules, with resorbed or poikilitically enclosed olivines (Figs. 1, 2, S1−S2, Friend et al., 2016). The third chondrule selected, Ch-2, was a POP chondrule showing radial zoning with an olivine- and (altered) mesostasis-rich interior and an outer zone dominated by low-Ca pyroxenes parallel to the surface (Fig. S3).

Chondrule olivine crystals appear homogeneous in back-scattered electron images (Fig. 2A, S2−S3) but high-resolution titanium X-ray maps reveal important chemical variations in the three chondrules (Fig. 2B, S1−S3). In some cases, these compositional variations occur within single crystals, with Ti-rich olivine engulfing Ti-poor olivine, implying overgrowth on a relict crystal (Fig. 2B). Ti-poor olivine grains are mainly located in the center of chondrule (Fig. 2B) but also occur as the center of olivine crystals dispersed throughout the chondrules (Fig. S2−S3). The overall zoning is comparable to the "inverse zonings" in some cathodoluminescence maps of porphyritic chondrules by (Pack et al., 2004; e.g. their Fig. 2D and 10B) and Kita et al. (2010). Outer-chondrule olivine crystals show oscillatory Ti zoning over thickness ranging from 10 to 30 µm (Fig. 2B, S2−S3), with a tendency to return to lower Ti contents (also seen at the edge of inner-chondrule crystals). This is the first time oscillatory zoning is reported in chondrule olivine (notwithstanding the single-oscillation high-FeO grain of Jacquet and Marrocchi, 2017) for elements other than the slow diffuser phosphorus (McCanta et al., 2016) although such zoning has long been described in pyroxene (e.g, Baecker et al., 2017; Jones, 1996). The overgrowths sometimes exhibit variable thicknesses, with thicker overgrowths toward the exterior of the chondrule (Fig. 2B). High-resolution quantitative analyses of olivine reveal trace element variations within each chondrule, with aluminum and titanium contents varying from 0.02 to 0.2 wt% and 0.01 to 0.08 wt%, respectively (Table S1). Importantly, both elements are positively correlated in PO chondrules (Fig. 3E and 4E, Tables S1 and S2) whereas the POP chondrule shows no specific correlation (Fig. S4E, Tables S1 and S2). Other well-defined correlations were observed in PO chondrules (Table S1 and S2): (i) Cr is positively correlated to Fe and Mn and negatively to the Mg# (= molar MgO/(MgO+FeO)), (ii) Fe is positive correlated with Mn.

A total of 118 SIMS spot analyses were performed in one session and used to assess oxygen isotope systematics of the three mapped and chemically characterized chondrules. Olivine O-isotope compositions plot along the PCM line with $\delta^{17}O$ and $\delta^{18}O$ ranging from –30.3 to +2.75‰ and from –27.3 to +5.1 ‰, respectively (Fig. 3A, 4A and S4A, Table S1). All chondrules show internal mass-independent O–isotope heterogeneity beyond analytical uncertainties, with $\Delta^{17}O$ varying by >5 ‰ (Fig. 3A, 4A and S4A, Table S1). Most of this variability is carried by Ti, Ca, Al-poor olivine grains whereas (varyingly) Ti, Ca, Al-richer grains cluster around the same $\Delta^{17}O$ value, producing "orthogonal" relationships (i.e. conjunction of an horizontal and a vertical trends) in $\Delta^{17}O$ vs. minor element plots (Fig. 3A, 4A, and S4). In each chondrule, the horizontal trend which regroups the majority of the grains can be taken as representing the host. That of the two PO chondrules ($\Delta^{17}O$ = –6.0 and –6.3 ‰) belongs to the ^{16}O-rich group of (Ushikubo et al., 2012) whereas the POP chondrule's ($\Delta^{17}O$ = –3.0 ‰) fits in the ^{16}O-poor one.

4- Discussion

4-1 Chemical characterization of relict olivines

Our high-resolution titanium X-ray maps of porphyritic chondrules reveal different populations of olivine grains characterized by variable titanium contents (Fig. 2B, S2−S3). Most Ti-poor olivine grains have oxygen isotopic compositions markedly distinct from their hosts (olivine grains with higher Ti concentrations; Fig. 3B, 4B and S4B, Tables S1 and S2). Following (Ushikubo et al., 2012), we consider olivines with $\Delta^{17}O$ deviating by >3σ from their host $\Delta^{17}O$ as relicts (host being the olivine grains showing homogeneous values with $\Delta^{17}O$ 2SD ≤ 1‰; Ushikubo et al., 2012). So most of these Ti-poor olivines are relict grains.

They may be ^{16}O-richer (Ch-2 and Ch-7) or ^{16}O-poorer (Ch-1) than their host olivine. Our results thus demonstrate that olivine Ti concentrations can constitute a *chemical* marker of relicts, in addition to isotopic data. Relict olivine grains are also systematically Al-poor (Fig. 3C, 4C and S4C, table S1) and, in one chondrule (Ch2), Ca-poor (Fig. 4D) relative to host olivines. However, relict olivine grains are not systemically depleted in Ca relative to the host (Table S1).

Ambiguity remains though regarding those Ti-poor olivine crystals with Δ^{17}O similar to the range defined by the host grains (Fig. 3, 4, S4, Table S1). Such grains could correspond to (i) relict grains with O-isotopic compositions coincidentally similar to host crystals or (ii) host olivine with lower Ti content relative to other host grains. Obvious relict olivine grains (i.e. with Δ^{17}O outside 3σ of the host), are mainly located in the center of chondrules (Fig. 5), whereas the aforementioned ambiguous grains occur at the outer edge of chondrules (Fig. 2, 5, S2−S3), suggesting an host origin (see also next subsection).

Our finding that relict chondrule olivine are Ca, Al, Ti-poor contrasts with the previous notion that refractory-*enriched* olivines were the relict grains (Pack et al., 2004; Pack and Palme, 2003) but even those workers had reported "inverse zonings" similar to those of this study when dealing with *bona fide* porphyritic chondrules (Pack et al., 2004). Since refractory forsterite crystals do occur independently in chondrites (Jacquet and Marrocchi, 2017; Pack et al., 2004), the possibility remains that some contributed to chondrule precursors although they were not found in this study.

At any rate, this study demonstrates that high-current EMPA mapping (at 500 nA) and quantitative analyses (at 900 nA) constitute a powerful method for characterizing relict olivine crystals as it allows very low detection limits for trace elements in olivine (≈10 ppm for Al, Ca, Mn & Ti; Sobolev et al., 2016) to be reached with limited interaction and emission volumes of X-rays in olivine grains (i.e., ≤6 μm^3; Batanova et al., 2015).

4-2 Origin of relict grains and nature of chondrule precursors

Coarse-grained olivine aggregates showing 120° triple junctions, such as in our PO chondrules analyzed, were interpreted by (Libourel and Krot, 2007) as potential fragments of differentiated planetesimals that experienced disruption early in the Solar System history. In such a scenario, all Mg-rich olivine grains would represent relict minerals that survived the chondrule-forming event(s). However, experimental samples with olivine triple junctions were produced during thermal annealing under nebular conditions, challenging the planetary origin of granoblastic olivine aggregates (GOA; Whattam and Hewins, 2009; Whattam et al., 2008). Our results show that large mass-independent O-isotope variations occur within chondrules showing triple junctions (Fig. 1). This does not support a planetary origin of GOA as crystallization from a magma ocean would result in very limited *and* mass-dependent O-isotopic fractionation (Richet et al., 1977). For instance, oxygen isotope compositions of primitive basaltic rocks vary within narrow ranges with mass-dependent fractionation limited to less than 1‰ (Eiler, 2001). Consequently, it appears that 120° triple junctions of olivines are not the result of lithostatic pressure (Whattam et al., 2008; Whattam and Hewins, 2009)—ours even seem to be shaped by overgrowths rather than the relicts themselves—arguing against a planetary origin of chondrules (Jacquet et al., 2012; Jacquet and Marrocchi, 2017). While derivation of neighboring relicts from *independent* planetary bodies remains unlikely but conceivable, known (macroscopic) achondrites sample a much more restricted range of O isotopic compositions (Greenwood et al., 2016).

The relict olivine grains in NWA 5958 are too poor in refractory elements to correspond to phenocrysts in refractory condensed melts as envisioned by (Pack et al., 2004). Their chemical features (Ca-Al-Ti-poor; Fig. 3, 4 & S4, Table S1) are however similar to olivine in amoeboid olivine aggregates (AOAs; Ruzicka et al., 2012; Sugiura et al., 2009;

Weisberg et al., 2004), which result from condensation from the nebular gas (Krot et al., 2004): for example AOA olivines in the same meteorite analyzed by Jacquet and Marrocchi (2017) have concentrations ranging 0.01-0.03 wt% TiO_2, 0.03-0.08 wt% Al_2O_3, comparable with our relicts (see section 4.1). Furthermore, olivines within individual AOAs commonly show variable $\Delta^{17}O$ values that could result from condensation under changing physical conditions (Krot et al., 2004). This support a kinship between AOAs and chondrule precursors, similar to that inferred for part of the precursors of agglomeratic chondrules in CR chondrites (Schrader et al., 2018). The presence of refractory inclusions among chondrule precursors is supported in the literature by the observation of (rare) relict CAIs and AOAs in chondrules (Aléon & Bourot-Denise, 2008; Krot et al. 2009; Yurimoto and Wasson 2002), aluminum-rich chondrules (Russell et al. 2000; Krot and Keil 2002) and volatility-fractionated rare earth element patterns in bulk chondrules (Misawa and Nakamura 1988; Jacquet and Marrocchi 2017 and references therein). However, chondrule precursors are unlikely to be solely AOAs as the latter are ^{16}O-rich ($\Delta^{17}O$ = –15 to –22 ‰; Krot et al., 2004) whereas relict olivine grains in NWA 5958 chondrules are isotopically diverse with $\Delta^{17}O$ ranging from –16.1 to +0.5‰ (Fig. 6, Table S1). Additionally, relict olivines in Ch-1 are enriched in $^{17,18}O$ relative to the host grains (Fig. 3, Table S1) and literature data indeed show relict olivine grains either enriched or depleted in ^{16}O relative to the host (Jones et al., 2004; Kita et al., 2010; Rudraswami et al., 2011; Tenner et al., 2015; 2013; Ushikubo et al., 2012). Since the oxygen isotopic characteristics of precursors should be better preserved than minor elements because of slower diffusion of oxygen: e.g., Ryerson et al., 1989), these cannot have been solely AOAs but were plausibly nebular condensates mineralogically analogous to them but characterized by a significant oxygen isotopic diversity. It is interesting to note that the analyzed relict olivines (Table 1) define a $\delta^{17}O$- $\delta^{18}O$ correlation (Fig. 6), described by $\delta^{17}O = (1.04\pm0.06) \times \delta^{18}O - (2.78\pm0.60)$ that is indistinguishable within errors from the PCM line

defined by SIMS measurements in chondrules (i.e., amalgamated host and relict data) from different carbonaceous chondrites (Ushikubo et al., 2012). The PCM line may thus have been already established in the chondrule precursors rather than being a result of chondrule formation, although some of the relicts (presumably among those in the range of host compositions) may be recycled chondrule debris.

We note that relict olivine grains are systematically studded with Fe-Ni metal beads (Fig. 2B). Such mineralogical associations could either result from (i) co-condensation of olivine and Fe-Ni metal beads, as observed in some AOAs (Krot et al., 2004) or (ii) sub-solidus reduction of FeO in olivine grains (Lemelle et al., 2001; Leroux et al., 2003). The latter produces peculiar textures with micron-sized Ni-poor (i.e., < 2 wt%) metal beads surrounded by silica-rich glass layers (Leroux et al., 2003) and defining lines in olivine crystals (Rambaldi, 1981), which are not observed in NWA 5958 chondrules (Fig. 2 and S2). If, on the contrary, the mineralogical association is pristine, the relicts must have condensed at a total pressure >10 Pa (i.e., 0.1 mbar) to produce Fe-Ni metal beads before condensation of Mg-rich olivine (Ebel, 2006; Ebel and Grossman, 2000; Petaev et al., 2005).

4-3 Chondrule melting and epitaxial growth of host olivine

The systematic Al-Ti-enrichments (and in some case in Ca, Fig. 4D) of host olivine grains compared to relicts suggest their formation from Ca-Al-Ti-melts (hereafter CAT-melts). Because the surviving relicts are (Ca)-Al-Ti-poor olivine, the melts generated upon heating should have been enriched in those elements compared to the bulk (more or less chondritic) precursor. Specifically, such melts could result from melting of CAI-like nodules and ribbons like those observed within AOAs, which are mainly composed of spinel, Ti-Ca-rich pyroxene and anorthite (Krot et al., 2004; Ruzicka et al., 2012; Weisberg et al., 2004).

Except spinel, all those phases have lower melting temperatures than Mg-rich olivine and their fusion during the high-temperature chondrule-forming event(s) would generate CAT-melts while preserving ^{16}O-rich spinel relicts as occasionally observed in type I chondrules (Rudraswami et al., 2011; Tenner et al., 2015; 2013; Ushikubo et al., 2012). According to equilibrium Ca-partitioning between forsterite and melt (Libourel, 1999) and the large range of CaO concentrations observed in PO chondrule mesostasis (i.e., 5-22 wt%, Jones and Scott, 1989; Libourel et al., 2006; Marrocchi and Libourel, 2013), the host olivine grains could present (i) similar Ca concentration than relict grains (e.g., Ch-1 and Ch-2, Table S1) or (ii) Ca-enrichment comparing to relicts (e.g., Ch-7; Fig. 4D, Table S1). In addition, sodium-enrichments in the CAT-melts would increase the degree of polymerization of the melt and the activity of CaO, thereby promoting the crystallization of Ca-rich host olivine (Libourel et al., 1999, Piani et al., 2016).

The presence of CAT-melt would then allow the crystallization of olivine overgrowths around the olivine relicts, by-passing the thermodynamic barrier of nucleation (Fokin et al., 2006). Such a process is attested by the textures of olivine grains inferred from Ti X-ray maps that reveal host-olivine crystallization on relict olivine grains *via* epitaxial growth (Fig. 2B). Such olivine subtraction from the melt would have further enriched the melt in incompatible elements, contributing to the Ca-Al-Ti-rich character of the overgrowths. Interestingly, Ca-Al-Ti-rich melt inclusions could be observed along the boundary between relict and host olivine grains (Fig. S1). Similar textures have been observed in terrestrial olivine phenocrysts that present olivine overgrowths on relict olivine cores (Sakyi et al., 2012), thus supporting the crystallization of chondrule host olivine grains *via* epitaxial growth on relict olivine grains inherited from chondrule precursors.

Because relicts are still visible in the X-ray maps, diffusion was not efficient enough to homogenize the olivine grains in Al and Ti. This runs counter to the batch crystallization

inferred by (Jacquet et al., 2015) and (Jacquet and Marrocchi, 2017) for type I chondrules, at least for this type of texture, in contradistinction to the largely homogeneous isolated refractory forsterites. For diffusion coefficients of order 10^{-14} m²/s in the temperature interval of olivine crystallization, the duration of this high-temperature episode must have been limited to no more than a few hours, though possibly not much shorter than this as e.g. Ca zonings appear significantly smoother and thus diffusion-affected.

4-4 Open system behavior

The enhanced thickness of host-olivine overgrowths near the periphery of the chondrules (Fig. 2B) indicates that olivine "nutrients" were sourced from outside, i.e. open system behavior. Indeed, the low Mg content of PO chondrule mesostases (<5 wt% MgO; Libourel et al., 2006; Marrocchi and Libourel, 2013) suggest that olivine may have become unstable in the CAT-melt and partially dissolved (Soulié et al., 2016)— it is also possible that the rounded to subhedral shapes of the relict olivines observed in NWA 5958 (Fig. 2B) reflect early such partial dissolutions (rather than only diffusive exchange with overgrowths). Under those conditions, further olivine crystallization may have required an influx of SiO and MgO from the gas phase. Such an influx has been invoked to account for the pyroxene-rich peripheries of porphyritic chondrules (Libourel et al., 2006; Piani et al., 2016; Marrocchi et al., 2016; Tissandier et al., 2002, Hezel et al., 2003, 2006; Krot et al. 2004; Friend et al. 2016) and thus may have similarly occurred during an earlier stage of chondrule crystallization. This is supported by the decreasing Ca, Al, and Ti contents of host olivine grains from the center toward the edge of chondrules (Fig. 2B) that likely results from the dilution of CAT-melts by gas-melt interactions (see Jacquet and Marrocchi, 2017). Our emerging scenario thus bears some similarity with the "Open System Fractional Crystallization" model of (Pack et al.,

2004), despite their different assumed (refractory) starting conditions. In such a scheme, the positive relationships between Al and Ti contents in olivine grains (Figs. 3E and 4E) simply reflect their common incompatibility in olivine, and their varied abundances (by at least a factor of 10; Table S1) would result from (i) the dilution of CAT-melts by incoming SiO and MgO from the gas phase and (ii) progressive crystallization of olivine, *concentrating* Al and Ti in the melt. The competition between these two processes may have produced the oscillatory character of some of the zoning.

While the Ca-Al-Ti contents of host olivine grains varied during chondrule formation, their O-isotope composition (i.e. $\Delta^{17}O$; Fig. 3B, 4B and S3B) remained constant. As the host-olivine O isotope composition nowhere approaches the mean of the observed relicts among the chondrules studied, rather than corresponding to the bulk precursor, must result from exchange with the gas. The O-isotopic composition of the gas must have been different for each chondrule, as host olivine grains in NWA 5958 show different average values ($\Delta^{17}O \approx -6$ and –3‰; Figs. 3B, 4B, and S3B; Jacquet and Marrocchi, 2017). These estimates are in agreement with those reported for different types of carbonaceous chondrites (Libourel and Chaussidon, 2011; Rudraswami et al., 2011; Tenner et al., 2015; 2013; Ushikubo et al., 2012), implying that within a single chondrite, chondrules formed in different environments of the protoplanetary disk with varying $\Delta^{17}O$ values (Tenner et al., 2015; 2013; Ushikubo et al., 2012). As chondrules in individual chondrites largely formed within a clan-specific reservoir (Jones, 2012), such variations occurred on limited spatial and/or temporal scales, e.g., owing to variable solid/gas mixing ratios.

5-Concluding remarks

We developed a method combining high-current electron microprobe X-ray mapping (at 500 nA) and quantitative measurements (at 900 nA) to determine the chemical characteristics of relict olivine grains in chondrules. They are Ca-Al-Ti-poor compared to their host olivine crystals and are mainly located in the center of chondrules. Ti-poor relict olivines show variable $\Delta^{17}O$ values in each chondrule, suggesting that chondrule precursors correspond to nebular condensates that formed under changing physical conditions but at pressures above 0.1 mbar. This holds in particular for GOAs with 120° triple junctions whose mass-independent O-isotope variations preclude a planetary origin.

The important chemical and O-isotope variations observed within each chondrule suggest that chondrules formed *via* melting of nebular precursors comprising olivine grains with varying $\Delta^{17}O$ values and CAI-like nodules and ribbons as those observed within AOAs. The resulting CAT-melts allowed subsequent epitaxial growth of Ca-Al-Ti-rich host-olivines on relict olivine grains. Incoming MgO and SiO from the gas phase induced (i) dilution of the CAT-melts, as attested by the positive Al-Ti correlation observed in chondrule olivine crystals, and (ii) buffering of the O-isotope compositions of chondrules, as attested by the constant $\Delta^{17}O$ values of host olivines. The O-isotopic variations between host olivine grains of different chondrules within a single chondrite demonstrate that the chondrules formed in different environments of the protoplanetary disk with different $\Delta^{17}O$ values, possibly due to variable solid/gas mixing ratios.

Acknowledgments

All the data used in the present article are available by contacting Yves Marrocchi. Laurent Tissandier, Andrey Gurenko and Mathieu Roskosz are thanked for helpful scientific discussions. Nordine Bouden is thanked for his assistance with isotopic measurements. We thanked Dominik Hezel and Ryoji Tanaka for constructive comments and Associate Editor Frederic Moynier for careful editing. This is CRPG-CNRS contribution #2564.

Figure captions

Fig. 1: Reflected-light optical images of chondrules (A) Ch-1 and (B) Ch-7 from CM-related chondrite NWA 5958. Schematic representations of olivine grains in chondrules (C) Ch-1 and (D) Ch-7 show the numerous 120° triple junctions (some indicated by red arrows) between Mg-rich olivine crystals.

Fig. 2: (A) Back-scattered electron image of PO chondrule Ch-1 in NWA 5958. Ol = olivine, lpx = low-Ca pyroxene, Fe-Ni = Fe-Ni metal beads and m = altered mesostasis. (B) X-ray map of the Ti distribution in Ch-1, revealing internal structures. Most olivine grains are composed of a Ti-poor core and an epitaxially grown Ti-rich olivine margin. Most Ti-poor olivine is located near the center of the chondrule, whereas outer olivine grains are enriched in Ti. Oscillatory Ti zoning and a decrease in Ti content are observed in peripheral olivine grains (see text).

Fig. 3: (A) Oxygen isotopic composition of olivine crystals in PO chondrule Ch-1 from chondrite NWA 5958, highlighting important mass-independent variations. The terrestrial fractionation line (TFL) and primary chondrule mineral line (PCM) are also drawn. Incompatible element concentrations plotted against $\Delta^{17}O$ reveal that relict olivine grains are systematically depleted in (B) TiO_2 and (C) Al_2O_3 relative to their host olivine crystals, which are characterized by variable concentrations of these elements. (D) Mg# vs. $\Delta^{17}O$, showing that relict olivine grains have lower iron contents than their host olivines. (E) The positive relationship between Al_2O_3 and TiO_2 in olivine grains (both oxide concentrations vary by at least a factor of 5) suggests a dilution effect due to incoming MgO and SiO from the gas phase (see section 4-2). (F) CaO vs. FeO concentrations in olivine grains.

Fig. 4: (A) Oxygen isotopic composition of olivine crystals in PO chondrule Ch-7 from chondrite NWA 5958. The terrestrial fractionation line (TFL) and primary chondrule minerals line (PCM) are drawn. $\Delta^{17}O$ vs. (B) TiO_2, (C) Al_2O_3, and (D) CaO in olivine are displayed. (E) Al_2O_3 vs. TiO_2 in olivine grains. (F) CaO vs. FeO in olivine crystals.

Fig. 5: (A) X-ray map of the Ti distribution showing the locations of ion probe measurements (colored circles). The color code indicates the deviation from the average $\Delta^{17}O$ value of the host olivine grains of this chondrule: $<3\sigma$ = blue, $3–6\sigma$ = green, $6–9\sigma$ = yellow, and $>9\sigma$ = red.

Fig. 6: Oxygen three-isotope plot showing the isotopic compositions of relict olivines from NWA 5958. The data define a linear trend that is indistinguishable, within errors, from the PCM line ($\delta^{17}O = [0.997\pm0.013] \times \delta^{18}O - [2.70\pm0.11]$; (Ushikubo et al., 2012)).

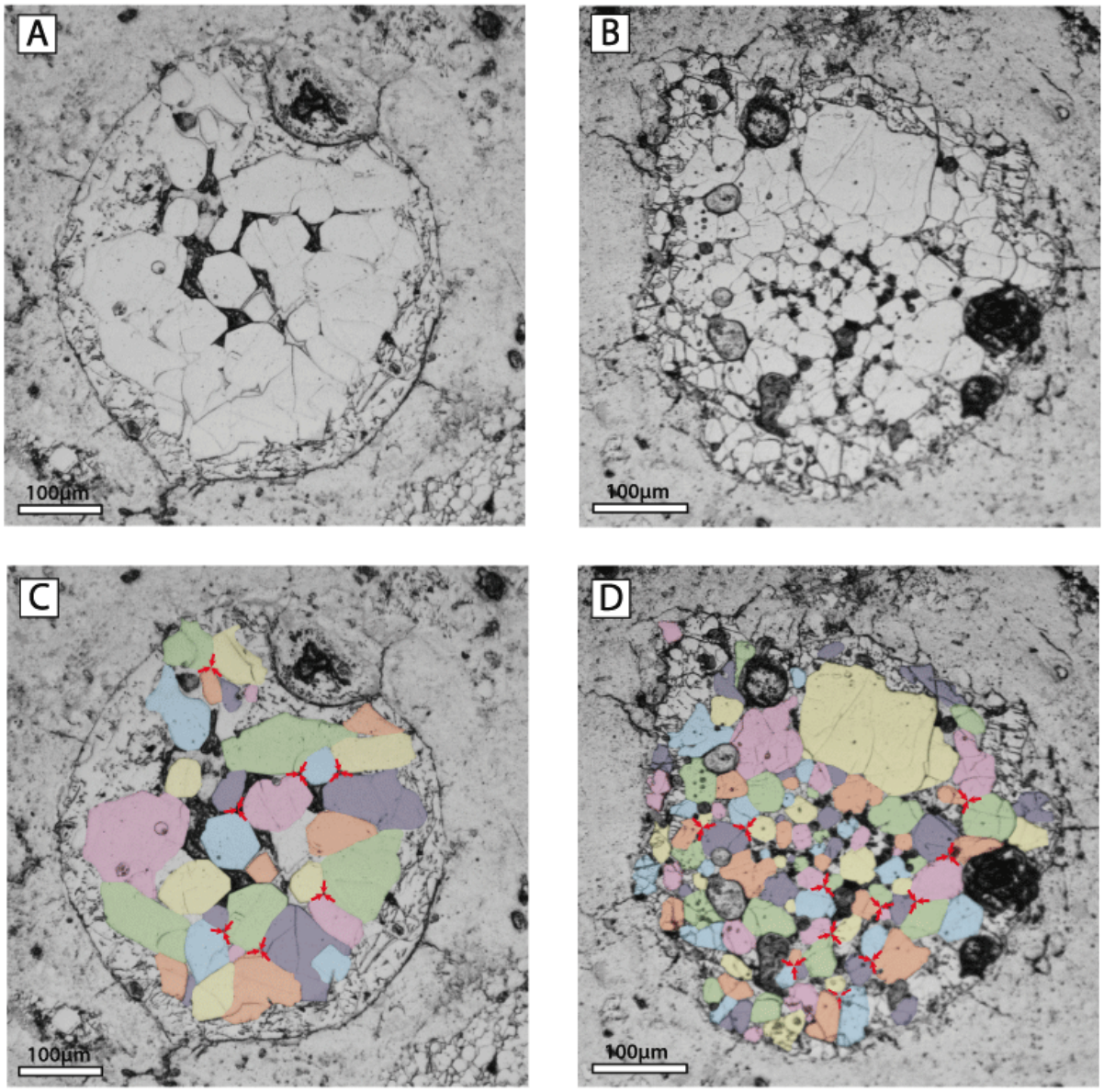

Fig. 1

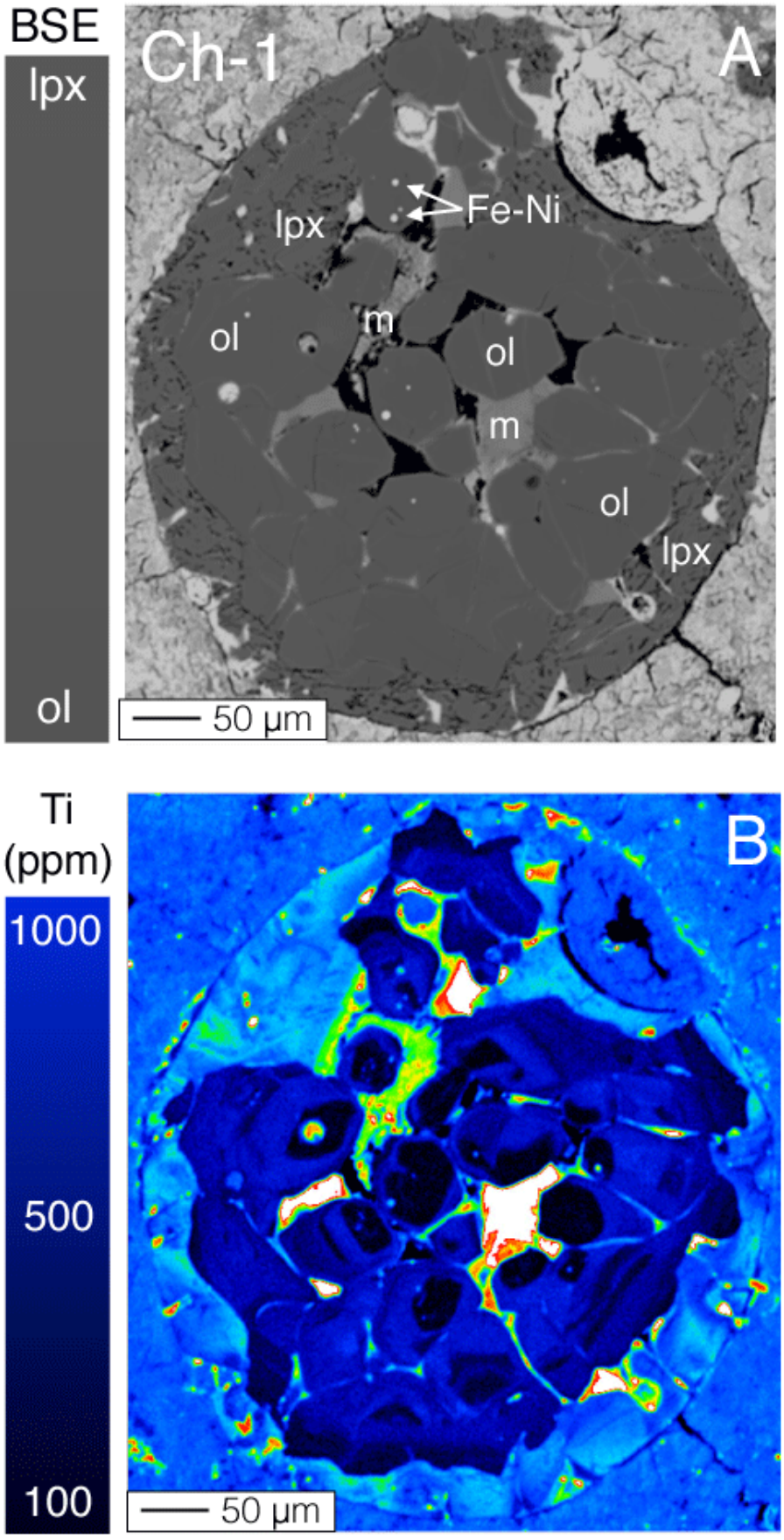
BSE
lpx
ol
Ch-1
A
lpx
Fe-Ni
ol
m
ol
m
ol
lpx
50 µm
Ti
(ppm)
1000
500
100
B
50 µm

Fig. 2

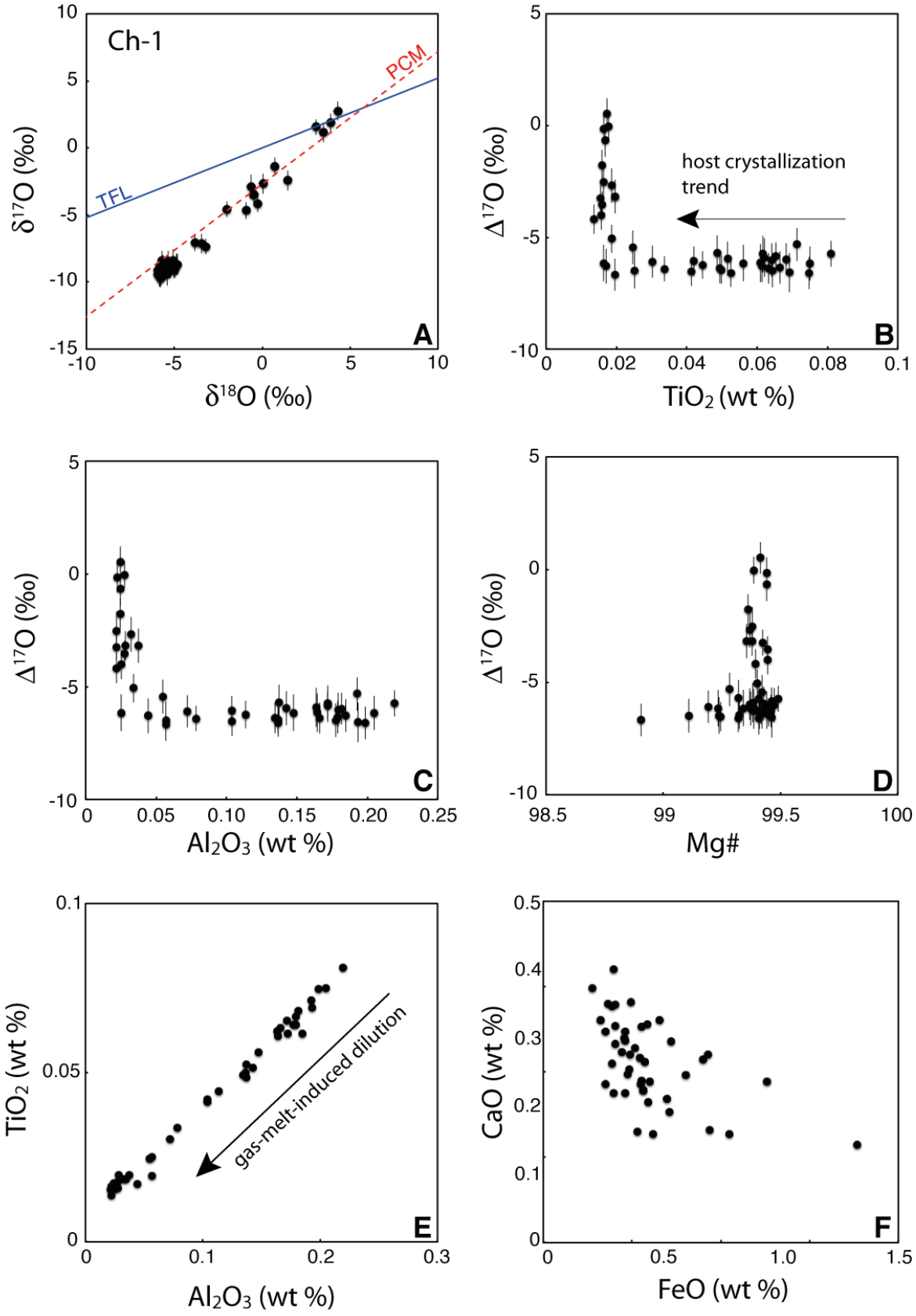
Ch-1
PCM
TFL
A
δ17O (‰)
δ18O (‰)
host crystallization
trend
B
Δ17O (‰)
TiO2 (wt %)
C
Al2O3 (wt %)
D
Mg#
E
gas-melt-induced dilution
F
CaO (wt %)
FeO (wt %)

Fig. 3

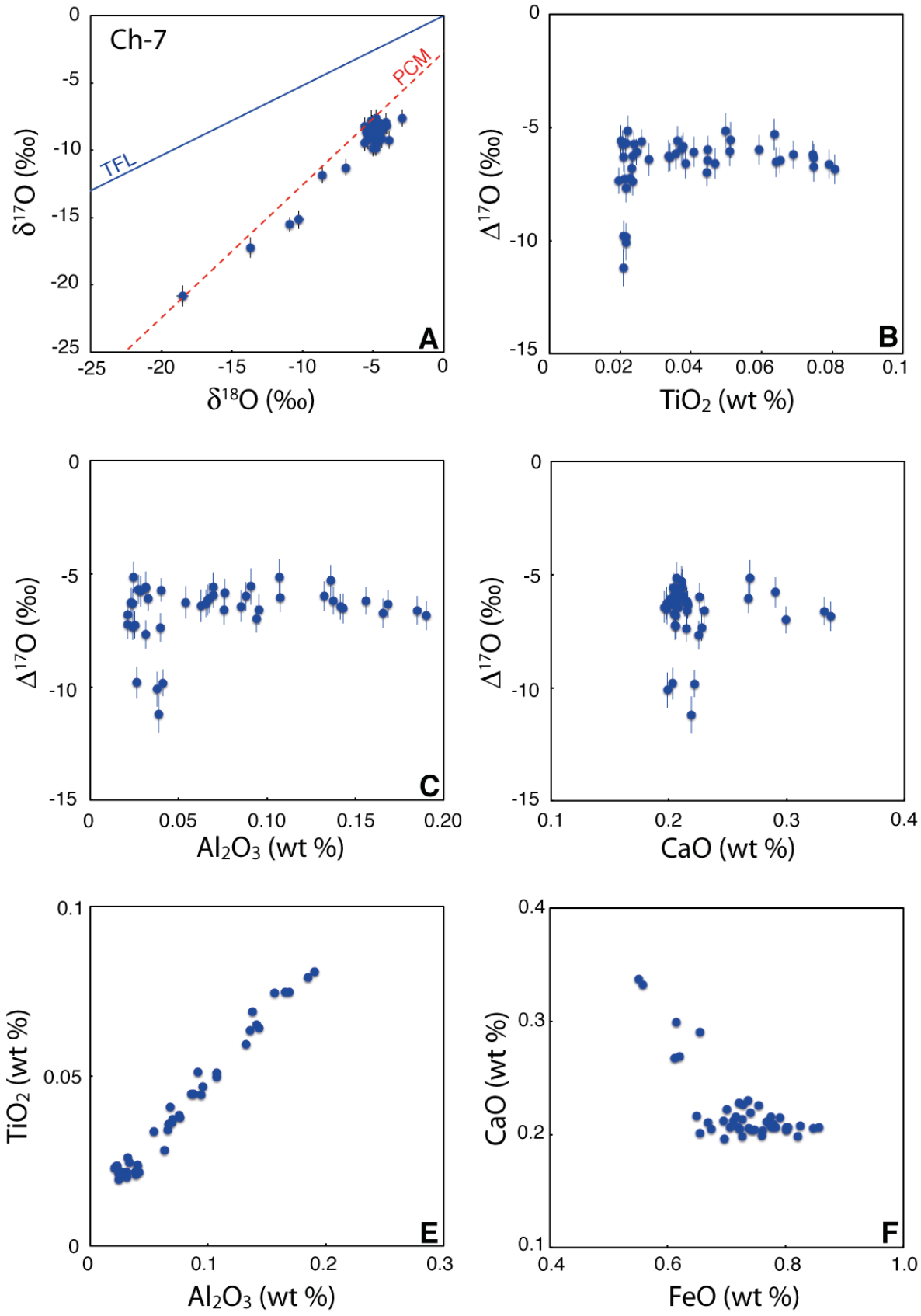
Ch-7
TFL
PCM
A
$\delta^{17}O$ (‰)
$\delta^{18}O$ (‰)
B
$\Delta^{17}O$ (‰)
TiO_2 (wt %)
C
$\Delta^{17}O$ (‰)
Al_2O_3 (wt %)
$\Delta^{17}O$ (‰)
CaO (wt %)
E
TiO_2 (wt %)
Al_2O_3 (wt %)
F
CaO (wt %)
FeO (wt %)

Fig. 4

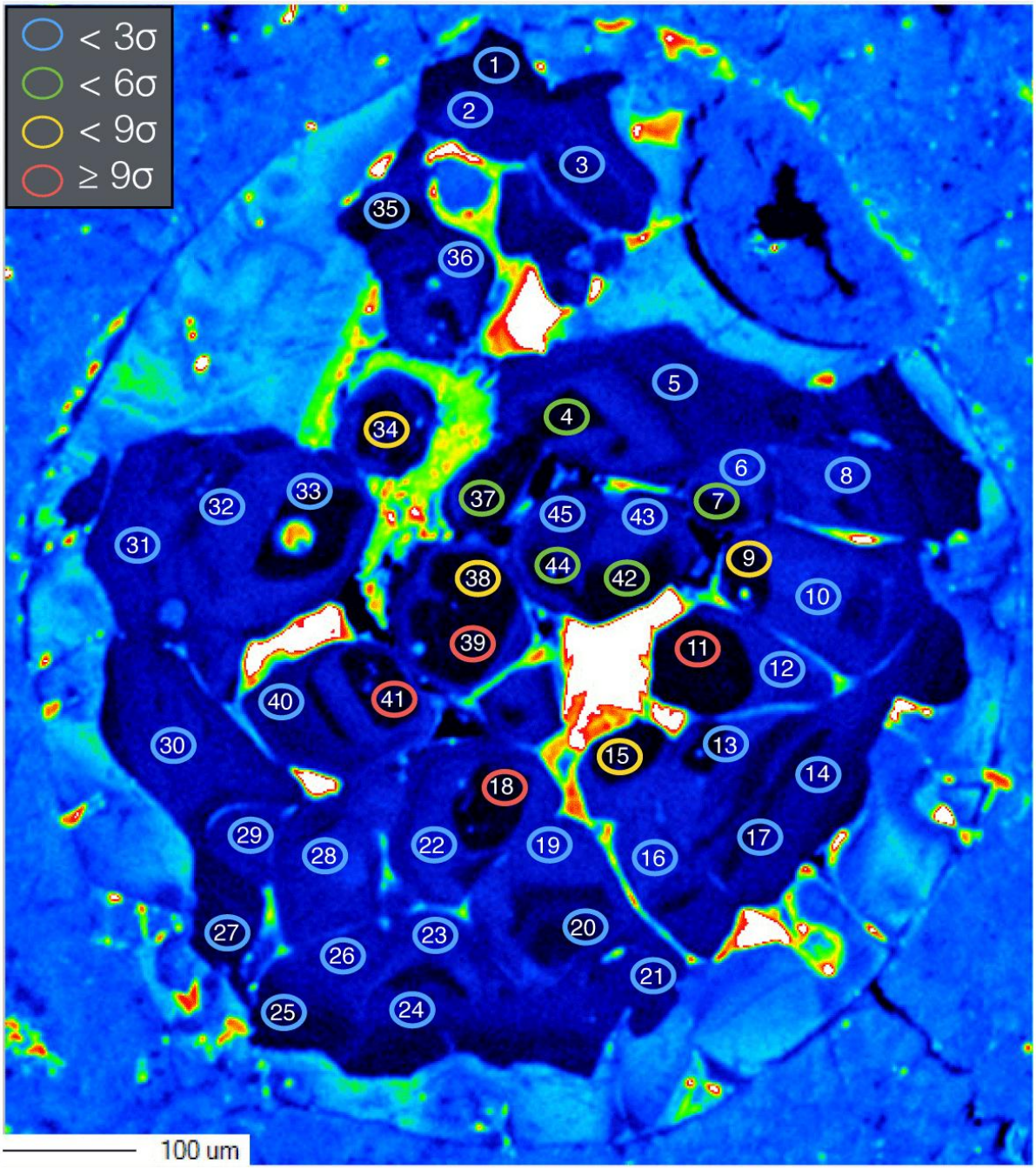
< 3σ
< 6σ
< 9σ
≥ 9σ
1
2
3
35
36
5
4
34
6
8
33
32
37
45
43
7
31
9
44
38
42
10
39
11
12
40
41
30
13
15
14
18
29
28
22
19
16
17
27
26
23
20
21
25
24
100 um

Fig. 5

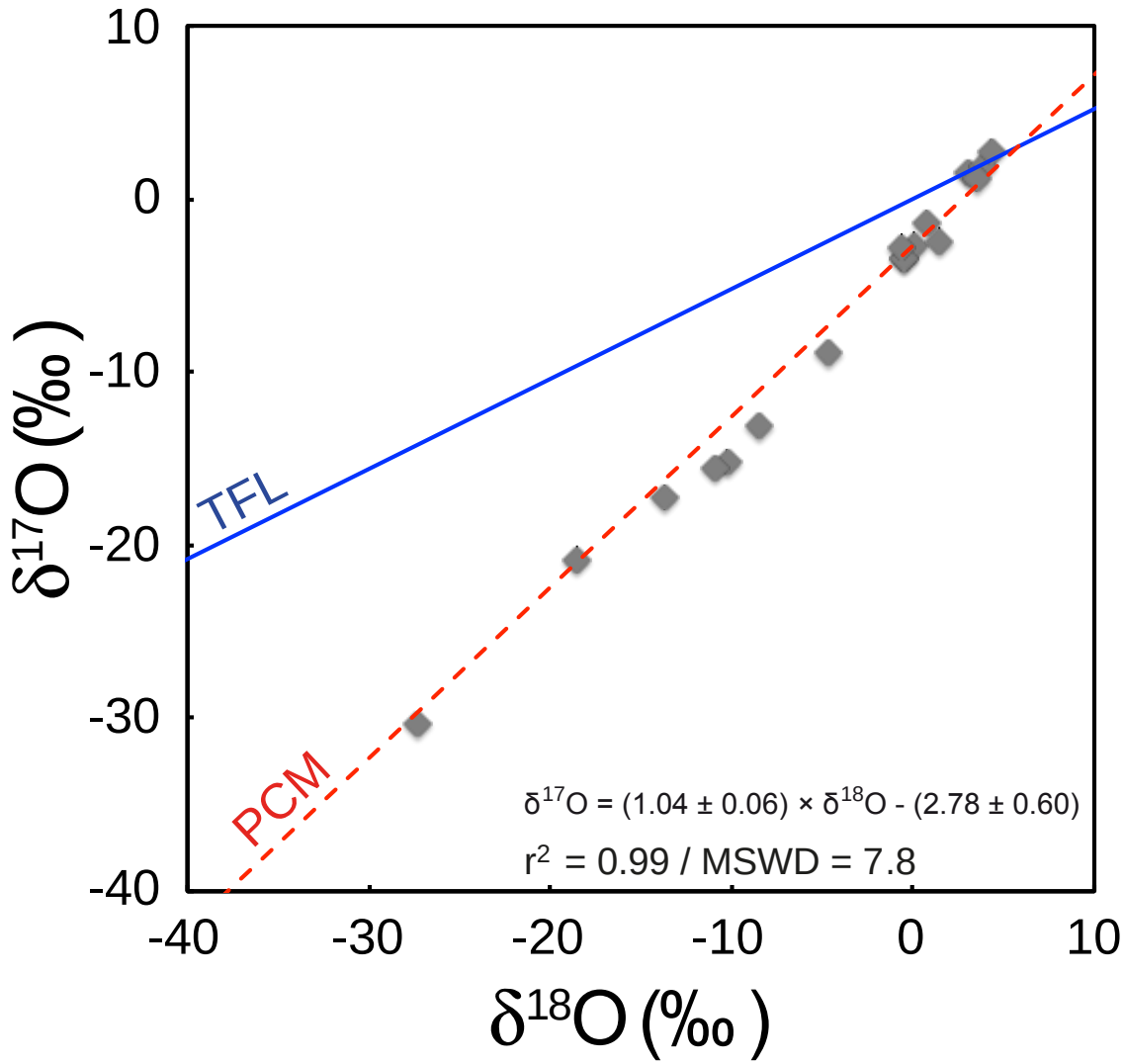
10
0
-10
-20
-30
-40
-40
-30
-20
-10
0
10
δ17O (‰)
δ18O (‰)
TFL
PCM
δ17O = (1.04 ± 0.06) × δ18O - (2.78 ± 0.60)
r2 = 0.99 / MSWD = 7.8

Fig. 6

chondrite	chondrule #	olivine type	n	$\delta^{18}O$ ‰	2σ	$\delta^{17}O$ ‰	2σ	$\Delta^{17}O$ ‰	2σ
NWA 5958	Ch-1 (PO)	host	35	-4.99	0.25	-8.61	0.71	-6.02	0.72
		relict		-0.48	0.22	-3.49	0.56	-3.24	0.57
		relict		0.05	0.25	-2.67	0.75	-2.69	0.76
		relict		3.06	0.26	1.56	0.59	-0.03	0.60
		relict		-0.46	0.28	-3.42	0.63	-3.18	0.65
		relict		3.90	0.26	1.87	0.66	-0.15	0.68
		relict		0.74	0.22	-1.39	0.68	-1.77	0.69
		relict		1.46	0.25	-2.42	0.75	-3.18	0.76
		relict		-0.63	0.28	-2.86	0.88	-2.54	0.89
		relict		4.30	0.25	2.75	0.68	0.52	0.70
		relict		3.49	0.25	1.15	0.72	-0.67	0.73
NWA 5958	Ch-7 (PO)	host	41	-4.90	0.23	-8.82	0.63	-6.27	0.64
		relict		-10.26	0.37	-15.15	0.68	-9.81	0.71
		relict		-10.91	0.26	-15.51	0.57	-9.83	0.59
		relict		-13.70	0.24	-17.23	0.76	-10.11	0.77
		relict		-18.49	0.42	-20.82	0.79	-11.20	0.82
NWA 5958	Ch-2 (POP)	host	25	1.97	0.26	-1.97	0.66	-3.00	0.67
		relict		-27.35	0.23	-30.34	0.63	-16.12	0.64
		relict		-4.63	0.27	-8.85	0.68	-6.44	0.69
		relict		-8.50	0.23	-13.16	0.65	-8.75	0.66

Table 1: Oxygen isotopic compositions of host and relict olivine grains in chondrules of chondrite NWA 5958. Relict grains correspond to those with low Ti contents and $\Delta^{17}O$ values outside 3σ of the average homogenous chondrule phase $\Delta^{17}O$ value (Ushikubo et al., 2012).

References

Aléon J. & Bourrot-Denise M., 2008, Mineralogy and petrography of a spectacular refractory inclusion that underwent chondrule formation (abstract #1638). 39th Lunar and Planetary Science Conference. CD-ROM.

Baecker, B., Rubin, A.E., Wasson, J.T., 2017. Secondary melting events in Semarkona chondrules revealed by compositional zoning in low-Ca pyroxene. Geochim. Cosmochim. Acta 211, 256–279. doi:10.1016/j.gca.2017.05.013

Batanova, V.G., Sobolev, A.V., Kuzmin, D.V., 2015. Trace element analysis of olivine: High precision analytical method for JEOL JXA-8230 electron probe microanalyser. Chemical Geology 419, 149–157. doi:10.1016/j.chemgeo.2015.10.042

Chaussidon, M., Libourel, G., Krot, A.N., 2008. Oxygen isotopic constraints on the origin of magnesian chondrules and on the gaseous reservoirs in the early Solar System. 72, 1924–1938. doi:10.1016/j.gca.2008.01.015

Clayton, R.N., 2003. Oxygen Isotopes in Meteorites, In Treatise on Geochemistry, Volume 1. Editor: Andrew M. Davis. Executive Editors: Heinrich D. Holland and Karl K. Turekian. 129-142. doi:10.1016/b0-08-043751-6/01063-x

Cohen, B.A., Hewins, R.H., Alexander, C.M.O., 2004. The formation of chondrules by open-system melting of nebular condensates. Geochim. Cosmochim. Acta 68, 1661–1675. doi:10.1016/j.gca.2003.09.009

Ebel, D.S., 2006. Condensation of rocky material in astrophysical environments. In Meteorites and the Early Solar System II, D. S. Lauretta and H. Y. McSween Jr. (eds.), University of Arizona Press, Tucson, 943 pp., p.253-277.

Ebel, D.S., Grossman, L., 2000. Condensation in dust-enriched systems. Geochim. Cosmochim. Acta 64, 339–366. doi:10.1016/s0016-7037(99)00284-7

Eiler, J.M., 2001. Oxygen Isotope Variations of Basaltic Lavas and Upper Mantle Rocks. Reviews in Mineralogy and Geochemistry 43, 319–364. doi:10.2138/gsrmg.43.1.319

Friend P., Hezel D.C., Mucershi D., 2016, The conditions of chondrule formation, Part II: Open System, Geochim. Cosmochim. Acta 173, 198-209.

Fokin, V.M., Zanotto, E.D., Yuritsyn, N.S., Schmelzer, J.W.P., 2006. Homogeneous crystal nucleation in silicate glasses: A 40 years perspective. Journal of Non-Crystalline Solids 352, 2681–2714. doi:10.1016/j.jnoncrysol.2006.02.074

Greenwood, R.C., Burbine, T.H., Miller, M.F., Franchi, I.A., 2016. Melting and differentiation of early-formed asteroids: The perspective from high precision oxygen isotope studies. Chemie der Erde - Geochemistry 1–43. doi:10.1016/j.chemer.2016.09.005

Hewins, R. H., Connolly, H. C., Logfren, G. E. J., and Libourel, G., 2005, Experimental Constraints on Chondrules Formation, Chondrites and the Protoplanetary Disk, ASP Conference Series, Vol. 341, San Fransisco: Astronomical Society of the Pacific, Hawai'i, p. 286.

Hezel D. C., Palme H., Brenker F. E., and Nasdala L. 2003. Evidence for fractional condensation and reprocessing at high temperatures in CH chondrites. Meteoritics & Planetary Science 38:1199–1215.

Hezel, D. C., Palme, H., Nasdala, L., and Brenker, F. E., 2006. Origin of SiO_2-rich components in ordinary chondrites. *Geochemica and Cosmochemica Acta* **70**, 1548-1564.

Hezel D.C., Palme H., 2007. The conditions of chondrule formation, Part 1: Closed system. Geochim. Cosmochim. Acta 71, 4092-4107. doi: 10.1016/j.gca.2007.06.035

Jacquet, E., Alard, O., Gounelle, M., 2015. Trace element geochemistry of ordinary chondrite chondrules: The type I/type II chondrule dichotomy. Geochim. Cosmochim. Acta 155, 47–67. doi:10.1016/j.gca.2015.02.005

Jacquet, E., Alard, O., Gounelle, M., 2012. Chondrule trace element geochemistry at the mineral scale. Meteoritics & Planetary Science 47, 1695-1714. doi:10.1111/maps.12005

Jacquet, E., Barrat, J.-A., Beck, P., Caste, F., Gattacceca, J., Sonzogni, C., Gounelle, M., 2016. Northwest Africa 5958: A weakly altered CM-related ungrouped chondrite, not a CI3. Meteorit Planet Sci 51, 851–869. doi:10.1111/maps.12628

Jacquet, E., Marrocchi, Y., 2017. Chondrule heritage and thermal histories from trace element and oxygen isotope analyses of chondrules and amoeboid olivine aggregates. Meteorit Planet Sci 58, 3451–23. doi:10.1111/maps.12985

Jones, R.H., 2012. Petrographic constraints on the diversity of chondrule reservoirs in the protoplanetary disk. Meteoritics & Planetary Science 47, 1176–1190. doi:10.1111/j.1945-5100.2011.01327.x

Jones, R.H., 1996. FeO-rich, porphyritic pyroxene chondrules in unequilibrated ordinary chondrites. Geochim. Cosmochim. Acta 60, 3115–3138. doi:10.1016/0016-7037(96)00152-4

Jones, R.H., Leshin, L.A., Guan, Y., Sharp, Z.D., 2004. Oxygen isotope heterogeneity in chondrules from the Mokoia CV3 carbonaceous chondrite. Geochim. Cosmochim. Acta 68, 3423–3438. doi:10.1016/j.gca.2004.01.013

Jones, R. H. and Scott, E. R. D., 1989, Petrology and thermal history of type IA chondrules in the Semarkona (LL3.0) chondrite, Lunar and Planetary Science Conference 19th, Lunar Planet. Inst., Houston, 523-536

Kimura, M., Grossman, J.N., Weisberg, M.K., 2011. Fe-Ni metal and sulfide minerals in CM chondrites: An indicator for thermal history. Meteoritics & Planetary Science 46, 431–442. doi:10.1111/j.1945-5100.2010.01164.x

Kita, N.T., Nagahara, H., Tachibana, S., Tomomura, S., Spicuzza, M.J., Fournelle, J.H., Valley, J.W., 2010. High precision SIMS oxygen three isotope study of chondrules in LL3 chondrites: Role of ambient gas during chondrule formation. Geochim. Cosmochim. Acta 74, 6610–6635. doi:10.1016/j.gca.2010.08.011

Krot A. N. and Keil K. 2002. Anorthite-rich chondrules in CR and CH carbonaceous chondrites: Genetic link between Ca, Al-rich inclusions and ferromagnesian chondrules.Meteoritics & Planetary Science 37:91–111.

Krot, A.N., Petaev, M.I., Russel, S.S., Itoh, S., Fagan, T.J., Yurimoto, H., Chizmadia, L., Weisberg, M.K., Komatsu, M., Ulyanov, A.A., Keil, K., 2004. Amoeboid olivine aggregates and related objects in carbonaceous chondrites: records of nebular and asteroid processes. Chemie der Erde - Geochemistry 64, 185–239. doi:10.1016/j.chemer.2004.05.001

Krot A. N., Amelin Y., Bland P., Ciesla F. J., Connelly J., Davis A. M., Huss G. R., Hutcheon I. D., Makide K., Nagashima K., Nyquist L. E., Russell S. S., Scott E. R. D., Thrane K., Yurimoto H., and Yin Q.-Z. 2009. Origin and chronology of chondritic components: A review. Geochimica et Cosmochimica Acta 73:4963–4997.

Kunihiro, Tak, Rubin, A.E., Wasson, J.T., 2005. Oxygen-isotopic compositions of low-FeO relicts in high-FeO host chondrules in Acfer 094, a type 3.0 carbonaceous chondrite closely related to CM. Geochim. Cosmochim. Acta 69, 3831–3840. doi:10.1016/j.gca.2005.01.031

Kunihiro, Takuya, Rubin, A.E., McKeegan, K.D., Wasson, J.T., 2004. Oxygen-isotopic compositions of relict and host grains in chondrules in the Yamato 81020 CO3.0 chondrite. Geochim. Cosmochim. Acta 68, 3599–3606. doi:10.1016/j.gca.2004.02.011

Lemelle, L., Guyot, F., Leroux, H., Libourel, G., 2001. An experimental study of the external reduction of olivine single crystals. American Mineralogist 86, 47–54. doi:10.2138/am-2001-0106

Leroux, H., Libourel, G., Lemelle, L., Guyot, F., 2003. Experimental study and TEM characterization of dusty olivines in chondrites: Evidence for formation by in situ reduction. Meteoritics & Planetary Science 38, 81–94. doi:10.1111/j.1945-5100.2003.tb01047.x

Libourel, G., 1999. Systematics of calcium partitioning between olivine and silicate melt: implications for melt structure and calcium content of magmatic olivines. Contrib Mineral Petrol 136, 63–80. doi:10.1007/s004100050524

Libourel, G., Chaussidon, M., 2011. Oxygen isotopic constraints on the origin of Mg-rich olivines from chondritic meteorites. Earth Planet. Sci. Lett. 301, 9–21. doi:10.1016/j.epsl.2010.11.009

Libourel, G., Krot, A., Tissandier, L., 2006. Role of gas-melt interaction during chondrule formation. Earth and Planetary Science Letters 251, 232–240. doi:10.1016/j.epsl.2006.09.011

Libourel, G., Krot, A.N., 2007. Evidence for the presence of planetesimal material among the precursors of magnesian chondrules of nebular origin. Earth and Planetary Science Letters 254, 1–8. doi:10.1016/j.epsl.2006.11.013

McCanta M.C., Beckett J.R. & Stolper E.M. (2016) Correlations and zoning patterns of phosphorous and chromium in olivine from H chondrites and the LL chondrite Sermakona. Meteoritics & Planetary Science 51, 520-546.

Marrocchi Y., Chaussidon M., Piani L. and Libourel G. (2016) Early scattering of the solar protoplanetary disk recorded in meteoritic chondrules. *Sci. Adv.* **2**, e1601001.

Marrocchi, Y., Bekaert, D.V., Piani, L., 2018. Origin and abundance of water in carbonaceous asteroids. Earth and Planetary Science Letters 482, 23–32. doi:10.1016/j.epsl.2017.10.060

Marrocchi, Y., Chaussidon, M., 2015. A systematic for oxygen isotopic variation in meteoritic chondrules. Earth Planet. Sci. Lett. 430, 308–315. doi:10.1016/j.epsl.2015.08.032

Marrocchi, Y., Libourel, G., 2013. Sulfur and sulfides in chondrules. Geochim. Cosmochim. Acta 119, 117–136. doi:10.1016/j.gca.2013.05.020

Misawa K. and Nakamura N. 1988. Demonstration of REE fractionation among individual chondrules from the Allende (CV3) chondrite. Geochimica et Cosmochimica Acta 52:1699–1710.

Nagahara, H., 1981. Evidence for secondary origin of chondrules. Nature 292, 135–136. doi:10.1038/292135a0

Pack, A., Palme, H., 2003. Partitioning of Ca and Al between forsterite and silicate melt in dynamic systems with implications for the origin of Ca, Al-rich forsterites in primitive meteorites. Meteoritics & Planetary Science 38, 1263‐1281. doi:10.1111/j.1945-5100.2003.tb00312.x

Pack, A., Palme, H., Shelley, J.M.G., 2005. Origin of chondritic forsterite grains. Geochim. Cosmochim. Acta 69, 3159–3182. doi:10.1016/j.gca.2005.01.013

Pack, A., Yurimoto, H., Palme, H., 2004. Petrographic and oxygen-isotopic study of refractory forsterites from R-chondrite Dar al Gani 013 (R3.5–6), unequilibrated ordinary and carbonaceous chondrites. Geochim. Cosmochim. Acta 68, 1135–1157. doi:10.1016/j.gca.2003.07.014

Petaev, M.I., Wood J.A., 2005. Meteoritic Constraints on Temperatures, Pressures, Cooling Rates, Chemical Compositions and Modes of Condensation in the Solar Nebula, In Chondrites and the Protoplanetary Disk, ASP Conference Series, Vol. 341, Proceedings of a workshop held 8-11 November 2004 in Kaua'i, Hawai'i. Edited by Alexander N. Krot, Edward R. D. Scott, and Bo Reipurth. San Francisco: Astronomical Society of the Pacific, p.373

Piani, L., Marrocchi, Y., Libourel, G., Tissandier, L., 2016. Magmatic sulfides in the porphyritic chondrules of EH enstatite chondrites. Geochim. Cosmochim. Acta 195, 84–99. doi:10.1016/j.gca.2016.09.010

Rambaldi, E.R., 1981. Relict grains in chondrules. Nature 293, 558–561. doi:10.1038/293558a0

Richet, P., Bottinga, Y., Javoy, M., 1977. A Review of Hydrogen, Carbon, Nitrogen, Oxygen, Sulphur, and Chlorine Stable Isotope Fractionation Among Gaseous Molecules. Annu. Rev. Earth Planet. Sci. 5, 65–110. doi:10.1146/annurev.ea.05.050177.000433

Rudraswami, N.G., Ushikubo, T., Nakashima, D., Kita, N.T., 2011. Oxygen isotope systematics of chondrules in the Allende CV3 chondrite: High precision ion microprobe studies. Geochim. Cosmochim. Acta 75, 7596–7611. doi:10.1016/j.gca.2011.09.035

Russell S. S., MacPherson G. J., Leshin L. A., and McKeegan K. D. 2000. ^{16}O enrichments in aluminum-rich chondrules from ordinary chondrites. Earth and Planetary Science Letters 184:57–74.

Russell, S.S., Krot, A.N., Huss, G.R, Keil K., Itoh S., Yurimoto H., MacPherson G.J., 2005, The genetic relationship between refractory inclusions and chondrules. In Chondrites and the Protoplanetary Disk, ASP Conference Series, Vol. 341, Proceedings of a workshop held 8-11 November 2004 in Kaua'i, Hawai'i. Edited by Alexander N. Krot, Edward R. D. Scott, and Bo Reipurth. San Francisco: Astronomical Society of the Pacific, 2005, p.317.

Ruzicka, A., Floss, C., Hutson, M., 2012. Amoeboid olivine aggregates (AOAs) in the Efremovka, Leoville and Vigarano (CV3) chondrites: A record of condensate evolution in the solar nebula. Geochim. Cosmochim. Acta 79, 79–105. doi:10.1016/j.gca.2011.11.043

Ruzicka, A., Hiyagon, H., Hutson, M., Floss, C., 2007. Relict olivine, chondrule recycling, and the evolution of nebular oxygen reservoirs. Earth and Planetary Science Letters 257, 274–289. doi:10.1016/j.epsl.2007.02.037

Ryerson, F.J., Durham, W.B., Cherniak, D.J., Lanford, W.A., 1989. Oxygen diffusion in olivine: Effect of oxygen fugacity and implications for creep. Journal of Geophysical Research 94, 4105–4118. doi:10.1029/JB094iB04p04105

Sakyi P.A., Tanaka R., Kobayashi K., Nakamura E., 2012. Inherited Pb isotopic records in olivine antercryst-hosted melt inclusions from Hawaiian lavas. Geochim. Cosmochim. Acta 95, 169-195.

Schrader, D.L., Connolly, H.C., Jr, Lauretta, D.S., Nagashima, K., Huss, G.R., Davidson, J., Domanik, K.J., 2013. The formation and alteration of the Renazzo-like carbonaceous chondrites II: Linking O-isotope composition and oxidation state of chondrule olivine. Geochim. Cosmochim. Acta 101, 302–327. doi:10.1016/j.gca.2012.09.045

Schrader, D.L., Connolly, H.C., Jr, Lauretta, D.S., Zega, T.J., Davidson, J., Domanik, K.J., 2015. The formation and alteration of the Renazzo-like carbonaceous chondrites III: Toward understanding the genesis of ferromagnesian chondrules. Meteorit Planet Sci 50, 15–50. doi:10.1111/maps.12402

Schrader, D.L., Nagashima, K., Waitukaitis, S.R., Davidson, J., McCoy, T.J., Connolly, H.C., Lauretta, D.S., 2018. The retention of dust in protoplanetary disks: Evidence from agglomeratic olivine chondrules from the outer Solar System. Geochim. Cosmochim. Acta 223, 405–421. doi:10.1016/j.gca.2017.12.014

Scott, E., Jones, R.H., 1990. Disentangling nebular and asteroidal features of C03 carbonaceous chondrite meteorites. exported from refbase Geochim. Cosmochim. Acta 54, 2485–2502. doi:10.1016/0016-7037(90)90235-d

Sobolev, A.V., Asafov, E.V., Gurenko, A.A., Arndt, N.T., Batanova, V.G., Portnyagin, M.V., Garbe-Schönberg, D., Krasheninnikov, S.P., 2016. Komatiites reveal a hydrous Archaean deep-mantle reservoir. Nature 531, 628–632. doi:10.1038/nature17152

Soulié, C., Libourel, G., Tissandier, L., 2016. Olivine dissolution in molten silicates: An experimental study with application to chondrule formation. Meteoritics & Planetary Science 52, 225–250. doi:10.1111/maps.12792

Sugiura, N., Petaev, M.I., Kimura, M., Miyazaki A., Hiyagon, H., 2009. Nebular history of amoeboid olivine aggregates. Meteoritics & Planetary Science 44, 559–572. doi:10.1111/j.1945-5100.2009.tb00751.x

Tenner, T.J., Nakashima, D., Ushikubo, T., Kita, N.T., Weisberg, M.K., 2015. Oxygen isotope ratios of FeO-poor chondrules in CR3 chondrites: Influence of dust enrichment and H2O during chondrule formation. Geochim. Cosmochim. Acta 148, 228–250. doi:10.1016/j.gca.2014.09.025

Tenner, T.J., Ushikubo, T., Kurahashi, E., Kita, N.T., Nagahara, H., 2013. Oxygen isotope systematics of chondrule phenocrysts from the CO3.0 chondrite Yamato 81020: Evidence for two distinct oxygen isotope reservoirs. Geochim. Cosmochim. Acta 102, 226–245. doi:10.1016/j.gca.2012.10.034.

Tenner T.J., Ushikubo T., Nakashima D., Schrader D.L., Weisberg M.K., Kimura M., Kita N.T. (In press) Oxygen Isotope Characteristics of Chondrules from Recent Studies by Secondary Ion Mass Spectrometry. In Chondrules and the protoplanetary disk. Cambridge University Press.

Tissandier, L., Libourel, G., Robert, F., 2002. Gas-melt interactions and their bearing on chondrule formation. Meteoritics & Planetary Science 37, 1377–1389. doi:10.1111/j.1945-5100.2002.tb01035.x

Ushikubo, T., Kimura, M., Kita, N.T., Valley, J.W., 2012. Primordial oxygen isotope reservoirs of the solar nebula recorded in chondrules in Acfer 094 carbonaceous chondrite. Geochim. Cosmochim. Acta 90, 242–264. doi:10.1016/j.gca.2012.05.010

Verdier-Paoletti, M.J., Marrocchi, Y., Avice, G., Roskosz, M., Gurenko, A., Gounelle, M., 2017. Oxygen isotope constraints on the alteration temperatures of CM chondrites. Earth Planet. Sci. Lett. 458, 273–281. doi:10.1016/j.epsl.2016.10.055

Weisberg, M.K., Connolly, H.C., Ebel, D.S., 2004. Petrology and origin of amoeboid olivine aggregates in CR chondrites. Meteoritics & Planetary Science 39, 1741–1753. doi:10.1111/j.1945-5100.2004.tb00070.x

Whattam, S.A., Hewins, R.H., 2009. Granoblastic olivine aggregates as precursors of Type I chondrules: An experimental test. Geochim. Cosmochim. Acta 73, 5460–5482. doi:10.1016/j.gca.2009.04.014

Whattam, S.A., Hewins, R.H., Cohen, B.A., Seaton, N.C., Prior, D.J., 2008. Granoblastic olivine aggregates in magnesian chondrules: Planetesimal fragments or thermally annealed solar nebula condensates? Earth and Planetary Science Letters 269, 200–211. doi:10.1016/j.epsl.2008.02.013

Yurimoto, H., Wasson, J.T., 2002. Extremely rapid cooling of a carbonaceous-chondrite chondrule containing very ^{16}O-rich olivine and a ^{26}Mg-excess. Geochim. Cosmochim. Acta 66, 4355–4363. doi:10.1016/s0016-7037(02)01218-8